Heliyon 9 (2023) e22267

Contents lists available at ScienceDirect

Heliyon

journal homepage: www.cell.com/heliyon

Research article

Simulating accurate and effective solutions of some nonlinear nonlocal two-point BVPs: Clique and QLM-clique matrix methods

Mohammad Izadi [a,*], Jagdev Singh [b], Samad Noeiaghdam [c,d]

[a] Department of Applied Mathematics, Faculty of Mathematics and Computer, Shahid Bahonar University of Kerman, Kerman, Iran
[b] Department of Mathematics, JECRC University, Jaipur-303905, Rajasthan, India
[c] Industrial Mathematics Laboratory, Baikal School of BRICS, Irkutsk National Research Technical University, Irkutsk, 664074, Russia
[d] Department of Applied Mathematics and Programming, South Ural State University, Lenin prospect 76, Chelyabinsk, 454080, Russia

ARTICLE INFO

MSC:
65L60
41A10
93B18
35J25
34B10

Keywords:
Clique functions
Collocation points
Elliptic BVPs
Nonlocal problems
Quasilinearization approach

ABSTRACT

This research work deals with two spectral matrix collocation algorithms based on (novel) clique functions to solve two classes of nonlinear nonlocal elliptic two-points boundary value problems (BVPs) arising in diverse physical models. The nonlinearity together with nonlocality makes the models so difficult to solve numerically. In both matrix methods by expanding the unknown solutions in terms of clique polynomials the nonlocality in the models is handled. In the first and direct technique, the clique coefficients are determined in an accurate way through solving an algebraic system of nonlinear equations. To get rid of the nonlinearity of the models and in order to gain efficacy, the quasilinearization method (QLM) is utilized in the second approach. In the latter algorithm named QLM-clique procedure, the first directly clique collocation method is applied to a family of linearized equations in an iterative manner. In particular, we show that the series expansion of clique polynomials is convergent exponentially in a weighted L_2 norm. Numerous numerical simulations validate the performance of two matrix collocation schemes and demonstrate the accuracy as well as the gain in computational efficiency in terms of elapsed CPU time. The proposed matrix algorithms for computation are easy to implement and straightforward, and provide more accuracy compared to other available computational values in the literature.

1. Introduction

There has been always an increasing interest in the study of boundary value problems (BVPs) for differential equations due to their importance in various disciplines of physical science and applied mathematics. The BVPs occur in the modeling of heat transfer, diffusion, chemical reactions, and the solution of optimal control problems [1,2].

In the current research study, we are concerned with numerical treatments of two classes of nonlinear nonlocal BVPs. To be precise, we are going to consider the following two models:

- Model problem (I): We consider the nonhomogeneous nonlocal BVPs reads [3,4]

* Corresponding author.
E-mail addresses: izadi@uk.ac.ir (M. Izadi), jagdevsinghrathore@gmail.com (J. Singh), snoei@istu.edu (S. Noeiaghdam).

https://doi.org/10.1016/j.heliyon.2023.e22267
Received 28 May 2023; Received in revised form 26 October 2023; Accepted 8 November 2023

Available online 13 November 2023
2405-8440/© 2023 The Author(s). Published by Elsevier Ltd. This is an open access article under the CC BY-NC-ND license (http://creativecommons.org/licenses/by-nc-nd/4.0/).

$$\begin{cases} -f\left(\int_0^1 \omega(p)dp\right)\frac{d^2}{d\tau^2}\omega(\tau) = g(\tau), \quad \tau \in \Omega_\tau := (0,1), \\ \omega(0) = \omega_0, \quad \omega(1) = \omega_1, \end{cases} \tag{1.1}$$

where ω_0, ω_1 are two given non-negative numbers. The previous work [3] addresses the issue of the existence and uniqueness of this model by means of fixed-point theory.

- Model problem (II): We study the nonlinear homogeneous nonlocal BVPs given as [4–6]

$$\begin{cases} -f\left(\int_0^1 \omega(p)dp\right)\frac{d^2}{d\tau^2}\omega(\tau) + \ell(\tau)\omega^{2n+1}(\tau) = 0, \quad \tau \in \Omega_\tau := (0,1), \\ \omega(0) = \omega_0, \quad \omega(1) = \omega_1, \end{cases} \tag{1.2}$$

where $n \in \mathbb{N}$ and ω_0, ω_1 belong to $[0, \infty)$. By means of Schauder's fixed-point theorem, the existence and the uniqueness issues of the model (II) with $l(\tau) \equiv 1$ were discussed and proved in [5].

In both models, the function $f = f(t)$ is a positive function of t, and g, ℓ are two given functions defined over Ω_τ. The above model problems (I) and (II) are called nonlocal due to the fact that the term $f\left(\int_0^1 \omega(p)dp\right)$ depends on the unknown $\omega(\tau)$ in the whole domain Ω_τ instead of a single point. The nonlocal BVPs of these types (1.1) and (1.2) play important roles in diverse branches of science such as the aeroelastic behavior of a flexible elastic suspended cable driven by mean wind speed [7] and thermo-viscoelastic flows [8], see [9] and references therein for more details.

Before describing the main contributions of this work, we provide a brief review of previously published work devoted to the model equations (1.1) and (1.2) numerically. Finite difference schemes were suggested in [3] and [6]. The variational iteration method (VIM) was developed in [4]. An optimal iterative method based on Green's functions and an optimal homotopy analysis method (GF-OHAM) has been studied in [10] and [11]. Finally, the Jacobi spectral method has been proposed recently in [12] to solve two models (I) and (II).

The spectral based collocation approaches are very common in simulating initial and BVPs. The benefit of spectral methods is that they provide a very accurate approximate solution for the model equations and achieve a higher accuracy with a low number of basis functions without employing discretization like the classical finite difference schemes. These methods have been successfully applied to a number of significant model problems with various (orthogonal) basis functions. Among these types of bases, we mention Morgan-Voyce [13], Vieta-Lucas [14], Bessel [15–17], Fibonacci [18], Jacobi [19], Chebyshev [20–24], and Vieta-Fibonacci [25], to name a few.

The focal objective of the present work is the development of two matrix collocation techniques based on clique functions [26–28]. Direct application of the spectral clique technique is accomplished in the first approach. Unlike the Jacobi spectral method [12], we describe a spectral algorithm in detail and in particular the convergence of the clique basis functions is established. The main advantage of this technique is that accurate approximate solutions are achieved using a few terms of the truncated series expansions. However, this approach suffers from the fact that by growing the number of bases, solving the corresponding nonlinear system is very time-consuming or we may not have convergence at all. The technique of quasilinearization (QLM) is then utilized in the second proposed approach to overcome this difficulty. Once the underlying model is transformed into a family of linearized BVPs, the direct spectral clique function acquires the approximate solution iteratively. This is the first time that two given models (I) and (II) are being solved by using the clique polynomials in two direct and iterative manners, to the best of the author's knowledge. Concisely speaking, the main features of the present research are highlighted as follows:

- Two classes of BVPs with nonlinearity and nonlocality and with numerous applications in diverse physical models are solved numerically by employing two matrix collocation algorithms based on novel clique functions.
- The first proposed approach is called the direct clique collocation method, which converts the model problems into nonlinear algebraic matrix equations, however, is more accurate than existing available well-established schemes such as VIM [4] and GF-OHAM [10,11].
- The second approach is called QLM-clique method, which is based on a combination of quasilinearization and the direct clique collocation method. This hybrid technique solves a sequence of linear subproblems and is more efficient and effective than the existing numerical schemes.
- The exponential convergence of the clique series expansion is proved in the L_2 norms theoretically and confirmed by defining the numerical order of convergence numerically in both proposed spectral methods.

The outline of this study is given next. In the next section, we first introduce some basic facts related to clique polynomials and also the convergence of these functions is established in a weighted L_2 norm. Then, in Section 3, we design two matrix collocation techniques based on the clique functions for two model equations (I) and (II) comprehensively. A detailed illustration of numerical simulations with three test cases is carried out in Section 4. Some concluding remarks are made in the final section.

2. Clique functions: basic matrix relations

Let's assume $\mathbb{G} := (V, E)$ is a (finite) graph, which is simple in the sense that has no multiple edges or loops. Here, V is the set of m vertices of $\mathbb{G}$ while E denotes the set of n edges of the graph. If two vertices are joined by a common edge in the graph, they are called adjacent vertices. We call $\mathbb{G}' = (V', E')$ a subgraph of $\mathbb{G}$ if we have $V' \subseteq V$ and $E' \subseteq E$. In a complete graph, all pair of vertices are adjacent. The complete graph with m vertices is shown by K_m, which has $\binom{m}{2}$ (undirected) edges. We define a q-clique in $\mathbb{G}$ to be a subgraph of $\mathbb{G}$ which is complete and has q vertices. For more information about graph theory, we refer to [29].

The concept of clique polynomials for a complete graph was first given in [30]. Denoting by $\mathbb{C}(\mathbb{G}, \tau)$, the clique polynomial of a given graph $\mathbb{G}$ is defined by

$$\mathbb{C}(\mathbb{G}, \tau) := \sum_{q=0}^{m} c_q(\mathbb{G})\, \tau^q,$$

where $c_q(\mathbb{G})$ denotes the number of q-cliques of $\mathbb{G}$ and $c_0(\mathbb{G}) = 1$. Whenever $V = \{\emptyset\}$, we set $\mathbb{C}(\mathbb{G}, \tau) := 1$. For a complete graph K_m, the number of distinct q-cliques is as $c_q(K_m) = \binom{m}{q}$. Thus, the related clique polynomials for K_m are rewritten as

$$\mathbb{C}_m(\tau) \equiv \mathbb{C}(K_m, \tau) := \sum_{q=0}^{m} \binom{m}{q} \tau^q. \tag{2.1}$$

For $m = 0, 1, 2, 3$, we get

$$\mathbb{C}_0(\tau) = 1,$$
$$\mathbb{C}_1(\tau) = 1 + \tau,$$
$$\mathbb{C}_2(\tau) = 1 + 2\tau + \tau^2,$$
$$\mathbb{C}_3(\tau) = 1 + 3\tau + 3\tau^2 + \tau^3.$$

We are interested in utilizing the clique polynomials of complete graphs on Ω_τ. To this end, we set

$$\mathbb{W}_M = \text{span}\langle \mathbb{C}_0(\tau), \mathbb{C}_1(\tau), \ldots, \mathbb{C}_M(\tau) \rangle,$$

as a finite subspace of

$$\mathcal{L}^2_w(\Omega_\tau) = \left\{ u : \Omega_\tau \to \mathbb{R} \ : \ u \text{ is measurable and } \|u\|_w < \infty \right\}.$$

Here, the related norm $\|\cdot\|$ and its weighing function are defined by

$$\|u\|^2_w = \int_{\Omega_\tau} |u(\tau)|^2\, w(\tau) d\tau, \quad w(\tau) := \frac{1}{|\Omega_\tau|}.$$

Obviously, $\mathbb{W}_M$ of finite dimensional $(M+1)$ is a closed subspace of $\mathcal{L}^2_w(\Omega_\tau)$. Thus, for an arbitrary function $u(\tau) \in \mathcal{L}^2_w(\Omega_\tau)$, one can find the finest (best) approximation $u_\star \in \mathbb{W}_M$ in the sense that

$$\|u(\tau) - u_\star(\tau)\|_w \le \|u(\tau) - v(\tau)\|_w, \quad \forall v \in \mathbb{W}_M. \tag{2.2}$$

We can expand an arbitrary function $u(\tau) \in \mathcal{L}^2_w(\Omega_\tau)$ as an infinite series in terms of clique polynomials $\mathbb{C}_m(\tau)$ in (2.1). However, we practically utilize a finite number of elements and restrict the discussion to the subspace $\mathbb{W}_M$. Therefore, we approximate $u(\tau)$ as follows

$$u(\tau) \approx u_M(\tau) = \sum_{m=0}^{M} p_m\, \mathbb{C}_m(\tau) = \boldsymbol{C}_M(\tau)\, \boldsymbol{P}_M, \quad \tau \in \Omega_\tau, \tag{2.3}$$

where

$$\boldsymbol{P}_M = \begin{bmatrix} p_0 & p_1 & \ldots & p_M \end{bmatrix}^T, \qquad \boldsymbol{C}_M(\tau) = \begin{bmatrix} \mathbb{C}_0(\tau) & \mathbb{C}_1(\tau) & \ldots & \mathbb{C}_M(\tau) \end{bmatrix}.$$

Here, we seek for the coefficients p_m as unknowns to be determined. We next define the error function $\mathcal{E}_M(\tau) = u(\tau) - u_M(\tau)$. The next result indicates that the norm of error tends to zero if we increase M. We recall that a function with r continuous derivatives is called a $C^{(r)}$ function.

Theorem 2.1. *Suppose that $u_M(\tau) = \boldsymbol{C}_M(\tau)\boldsymbol{P}_M$ denotes the best approximation to $u(\tau)$ in the space $\mathbb{W}_M$ and let $u \in C^{(M+1)}(\bar{\Omega}_\tau) \cap \mathcal{L}^2_w(\Omega_\tau)$. Then, it holds*

$$\|\mathcal{E}_M(\tau)\|_w \le \frac{\|u\|_{\infty, M+1}\, \mathcal{T}_0^{M+1}}{(M+1)!},$$

where $\|u\|_{\infty, M} := \sup_{\tau \in \bar{\Omega}_\tau} |u^{(M)}(\tau)|$ and $\mathcal{T}_0 = \max\{\tau_0, 1 - \tau_0\}$ for a $\tau_0 \in \bar{\Omega}_\tau$.

Proof. We first select an arbitrary point $\tau_0 \in \bar{\Omega}_\tau$. We now expand the function $u(\tau)$ about τ_0 giving us the following representation

$$u(\tau) = u(\tau_0) + (\tau - \tau_0)u'(\tau_0) + (\tau - \tau_0)^2 u''(\tau_0)/2! + \ldots + (\tau - \tau_0)^M u^{(M)}(\tau_0)/M! + R_{M+1}(\tau),$$

where $R_{M+1}(\tau) = (\tau - \tau_0)^{M+1} u^{(M+1)}(s_\tau)/(M+1)!$ denotes the remainder error term and s_τ is between τ_0 and τ. By defining $U_M(\tau) = \sum_{j=0}^{M} (\tau - \tau_0)^j u^{(j)}(\tau_0)/j!$, it is known from calculus theory [31] that the residual error satisfies

$$|u(\tau) - U_M(\tau)| = |R_{M+1}(\tau)| \leq \frac{\mathcal{T}_0^{M+1} \|u\|_{\infty,M+1}}{(M+1)!}. \tag{2.4}$$

Due to (2.2), we know that $u_M(\tau)$ is the finest approximation out of $\mathbb{W}_M$ to $u(\tau)$. So, we get

$$\|\mathcal{E}_M(\tau)\|_w^2 \leq \|u(\tau) - v(\tau)\|_w^2, \quad \forall v \in \mathbb{W}_M.$$

It is sufficient to select $v(\tau) = U_M(\tau) \in \mathbb{W}_M$ in the foregoing inequality to obtain

$$\|\mathcal{E}_M(\tau)\|_w^2 \leq \|u(\tau) - U_M(\tau)\|_w^2 = \int_{\Omega_\tau} |u(\tau) - U_M(\tau)|^2 w(\tau) d\tau.$$

If we use the result derived in (2.4), we arrive at

$$\|\mathcal{E}_M(\tau)\|_w^2 \leq \int_{\Omega_\tau} \left| \frac{\mathcal{T}_0^{M+1} \|u\|_{\infty,M+1}}{(M+1)!} \right|^2 w(\tau) d\tau \leq \left| \frac{\mathcal{T}_0^{M+1} \|u\|_{\infty,M+1}}{(M+1)!} \right|^2 \int_{\Omega_\tau} w(\tau) d\tau.$$

The proof is completed by noting that $\int_{\Omega_\tau} w(\tau) d\tau = 1$ followed by taking the square root from both sides of the last relation. □

It is also not a difficult task to show that the vector of clique polynomials $\boldsymbol{C}_M(\tau)$ in (2.3) can be written as

$$\boldsymbol{C}_M(\tau) = \boldsymbol{\chi}_M(\tau) \boldsymbol{K}_M, \tag{2.5}$$

where $\boldsymbol{\chi}_M(\tau)$ as the vector of monomials is given by

$$\boldsymbol{\chi}_M(\tau) = \begin{bmatrix} 1 & \tau & \tau^2 & \ldots & \tau^M \end{bmatrix},$$

and $\boldsymbol{K}_M$ as a lower-triangular matrix is defined by

$$\boldsymbol{K}_M = \begin{pmatrix} \binom{0}{0} & \binom{1}{0} & \binom{2}{0} & \cdots & \binom{M-1}{0} & \binom{M}{0} \\ 0 & \binom{1}{1} & \binom{2}{1} & \cdots & \binom{M-1}{1} & \binom{M}{1} \\ 0 & 0 & \binom{2}{2} & \cdots & \binom{M-1}{2} & \binom{M}{2} \\ \vdots & \vdots & \ddots & \ddots & \ddots & \vdots \\ 0 & & & \cdots & \binom{M-1}{M-1} & \binom{M}{M-1} \\ 0 & & & \cdots & & \binom{M}{M} \end{pmatrix}_{(M+1)\times(M+1)}.$$

It can be clearly seen that $\det(\boldsymbol{K}_M) = \prod_{j=0}^{M} \binom{j}{j}$, which is equal to one. Therefore, $\boldsymbol{K}_M$ in an invertible matrix.

On account of two former relations (2.3) and (2.5), we may express the approximated solution $u_M(\tau)$ as

$$u_M(\tau) = \boldsymbol{\chi}_M(\tau) \boldsymbol{K}_M \boldsymbol{P}_M. \tag{2.6}$$

One can also prove that the derivatives of $\boldsymbol{\chi}_M(\tau)$ namely $\frac{d^\nu}{d\tau^\nu} \boldsymbol{\chi}_M(\tau)$ are written in terms of itself. To be more precise, we have

$$\frac{d^\nu}{d\tau^\nu} \boldsymbol{\chi}_M(\tau) = \boldsymbol{\chi}_M(\tau) (\boldsymbol{E}_M)^\nu, \quad \boldsymbol{E}_M = \begin{pmatrix} 0 & 1 & 0 & \ldots & 0 \\ 0 & 0 & 2 & \ldots & 0 \\ \vdots & \vdots & \ddots & \vdots & \vdots \\ 0 & 0 & 0 & \ddots & M \\ 0 & 0 & 0 & \ldots & 0 \end{pmatrix}_{(M+1)\times(M+1)}, \tag{2.7}$$

for $\nu = 1, 2$. Indeed, $\boldsymbol{E}_M$ is called the differentiation matrix. A set of collocation points on Ω_τ must be given to obtain the numerical solutions of BVPs (1.1) as well as (1.2). Instead of an uniform partitioning of Ω_τ, we use the shifted zeros of the Chebyshev nodes given in the following

$$\tau_\xi = \frac{1}{2}(1 - x_\xi), \quad \xi = 1, 2, \ldots, M+1, \tag{2.8}$$

where $x_\xi := \cos\left(\frac{2\xi - 1}{M+1} \frac{\pi}{2}\right)$ are the roots of the classical Chebyshev functions of the first kind.

3. Two matrix collocation techniques

We will propose two matrix collocation algorithms using the clique basis functions to solve the linear and nonlinear model problems (I) and (II) in (1.1) and (1.2) respectively. While the first procedure is applied directly to these models, in the second approach we first utilize the technique of quasilinearization to convert the nonlinear nonlocal equation (1.2) into a family of simpler model equations. We illustrate these algorithms in detail below.

3.1. Directly proposed approach

Supposedly, we can express the solution $\omega(\tau)$ of model (I) and (II) in terms of clique functions. In view of (2.3), (2.5), and (2.6) we can write

$$\omega(\tau) \approx \mathcal{W}_M(\tau) = \sum_{m=0}^{M} p_m \, \mathbb{C}_m(\tau) = \boldsymbol{\chi}_M(\tau) \boldsymbol{K}_M \boldsymbol{P}_M, \quad \tau \in \Omega_\tau, \tag{3.1}$$

in which we have used $\boldsymbol{\chi}_M(\tau) = \begin{bmatrix} 1 & \tau & \tau^2 & \dots & \tau^M \end{bmatrix}$, $\boldsymbol{K}_M$ is defined in the last section, and

$$\boldsymbol{P}_M = \begin{bmatrix} p_0 & p_1 & \dots & p_M \end{bmatrix}^T, \qquad \boldsymbol{C}_M(\tau) = \begin{bmatrix} \mathbb{C}_0(\tau) & \mathbb{C}_1(\tau) & \dots & \mathbb{C}_M(\tau) \end{bmatrix}.$$

By using the former relations (2.3)-(2.6), we may express $\mathcal{W}_M(\tau)$ as

$$\mathcal{W}_M(\tau) = \boldsymbol{C}_M(\tau) \boldsymbol{P}_M = \boldsymbol{\chi}_M(\tau) \boldsymbol{K}_M \boldsymbol{P}_M. \tag{3.2}$$

In the latter relation, we differentiate twice with regard to variable τ. Utilizing the relation (2.7) to get

$$\begin{cases} \mathcal{W}_M^{(1)}(\tau) = \boldsymbol{\chi}_M(\tau) \boldsymbol{E}_M \boldsymbol{K}_M \boldsymbol{P}_M, \\ \mathcal{W}_M^{(2)}(\tau) = \boldsymbol{\chi}_M(\tau) (\boldsymbol{E}_M)^2 \boldsymbol{K}_M \boldsymbol{P}_M. \end{cases} \tag{3.3}$$

The following theorem states the ways that the approximate solutions $\mathcal{W}_M(\tau)$ and $\frac{d^2}{d\tau^2}\mathcal{W}_M(\tau)$ can be written in the matrix forms. We proceed by defining the following vectors

$$\boldsymbol{X} = \begin{pmatrix} \boldsymbol{\chi}_M(\tau_1) \\ \boldsymbol{\chi}_M(\tau_2) \\ \vdots \\ \boldsymbol{\chi}_M(\tau_{M+1}) \end{pmatrix}, \quad \boldsymbol{W} = \begin{pmatrix} \mathcal{W}_M(\tau_1) \\ \mathcal{W}_M(\tau_2) \\ \vdots \\ \mathcal{W}_M(\tau_{M+1}) \end{pmatrix}, \quad \boldsymbol{W}^{(2)} = \begin{pmatrix} \mathcal{W}_M^{(2)}(\tau_1) \\ \mathcal{W}_M^{(2)}(\tau_2) \\ \vdots \\ \mathcal{W}_M^{(2)}(\tau_{M+1}) \end{pmatrix}. \tag{3.4}$$

Theorem 3.1. *The matrix representation forms of* $\frac{d^\nu}{d\tau^\nu}\mathcal{W}_M(\tau)$, $\nu = 0, 2$ *at the Chebyshev nodes* (2.8) *are given by*

$$\boldsymbol{W} = \boldsymbol{X}_M \boldsymbol{K}_M \boldsymbol{P}_M, \tag{3.5}$$

$$\boldsymbol{W}^{(2)} = \boldsymbol{X}_M (\boldsymbol{E}_M)^2 \boldsymbol{K}_M \boldsymbol{P}_M. \tag{3.6}$$

Proof. The main idea of proof is to place the points (2.8) into relations (3.2)-(3.3) followed by utilizing the defined vectors (3.4). □

Since the considered models involve an integral term, one needs to approximate it in the matrix form. To do so, we integrate the relation (3.2) over Ω_τ to get

$$\int_{\Omega_\tau} \mathcal{W}_M(p) dp = \left(\int_{\Omega_\tau} \boldsymbol{\chi}_M(p) \right) \boldsymbol{K}_M \boldsymbol{P}_M = \boldsymbol{I}_M \boldsymbol{K}_M \boldsymbol{P}_M, \tag{3.7}$$

where the constant vector $\boldsymbol{I}_M$ as the integral of $\boldsymbol{\chi}_M(p)$ is $I_M := \begin{bmatrix} 1 & \frac{1}{2} & \frac{1}{3} & \dots & \frac{1}{M+1} \end{bmatrix}$.

3.1.1. The nonhomogeneous nonlocal model problem (I)

We proceed by inserting the set of Chebyshev nodes (2.8) into the model (1.1) to arrive at

$$-f\left(\int_0^1 \mathcal{W}_M(p) dp \right) \frac{d^2}{d\tau^2} \mathcal{W}_M(\tau_\xi) = g(\tau_\xi), \quad \xi = 1, 2, \dots, M+1, \tag{3.8}$$

where we have replaced $\omega(\tau)$ by its approximation $\mathcal{W}_M(\tau)$. By using the matrix notations (3.6) and (3.7), we rewrite the latter equations (3.8) compactly as

$$-f\left(\boldsymbol{I}_M \boldsymbol{K}_M \boldsymbol{P}_M \right) \boldsymbol{W}^{(2)} = \boldsymbol{G}. \tag{3.9}$$

Here, the right-hand-side vector $\boldsymbol{G}$ is given by

$$\boldsymbol{G}=\begin{pmatrix} g(\tau_1)\\ g(\tau_2)\\ \vdots\\ g(\tau_{M+1})\end{pmatrix}_{(M+1)\times 1}.$$

We now get the fundamental matrix equation by placing the relation (3.6) into the former equation (3.9) as

$$\boldsymbol{H}\,\boldsymbol{P}_M=\boldsymbol{G},\qquad \text{or}\quad [\boldsymbol{H};\boldsymbol{G}], \tag{3.10}$$

where

$$\boldsymbol{H}:=\left\{-f\left(\boldsymbol{I}_M\,\boldsymbol{K}_M\,\boldsymbol{P}_M\right)\boldsymbol{X}_M\,(\boldsymbol{E}_M)^2\right\}\boldsymbol{K}_M.$$

It can be readily seen that we need to solve a nonlinear matrix equation, which its degree of nonlinearity depends strictly on the positive function f. In the numerical part, different kinds of this function are considered. Besides, we use the nonlinear solver of Newton type to solve the nonlinear system (3.10).

3.1.2. The homogeneous nonlinear nonlocal model problem (II)

Similar to the first linear model (I), we consider the relation (1.2). By inserting the set of Chebyshev nodes (2.8) into it to get

$$-f\left(\int_0^1 \mathcal{W}_M(p)dp\right)\frac{d^2}{d\tau^2}\mathcal{W}_M(\tau_\xi)+\ell(\tau_\xi)(\mathcal{W}_M)^{2n+1}(\tau_\xi)=0,\quad \xi=1,2,\dots,M+1. \tag{3.11}$$

We next introduce the matrix $\boldsymbol{L}$ in the diagonal form and the zero vector $\boldsymbol{Z}$ as

$$\boldsymbol{L}=\begin{pmatrix} \ell(\tau_1) & 0 & \dots & 0\\ 0 & \ell(\tau_2) & \dots & 0\\ \vdots & \vdots & \ddots & \vdots\\ 0 & 0 & \dots & \ell(\tau_{M+1})\end{pmatrix},\quad \boldsymbol{Z}=\begin{pmatrix}0\\0\\ \vdots\\0\end{pmatrix}.$$

Therefore, we now able to rewrite the system of equations (3.11) in a compact representation form as

$$-f\left(\boldsymbol{I}_M\,\boldsymbol{K}_M\,\boldsymbol{P}_M\right)\boldsymbol{W}^{(2)}+\boldsymbol{L}\,\boldsymbol{W}^{2n+1}=\boldsymbol{Z}, \tag{3.12}$$

where the vectors $\boldsymbol{W}$ and $\boldsymbol{W}^{(2)}$ are defined in (3.4).

Remark 3.2. The powers of $\boldsymbol{W}$ in (3.12) can be handled in a matrix form by a recursive manner. To treat the term $\boldsymbol{W}^2$, we use the following relation

$$\boldsymbol{W}^2=\begin{pmatrix}\mathcal{W}_M^2(\tau_1)\\ \mathcal{W}_M^2(\tau_2)\\ \vdots\\ \mathcal{W}_M^2(\tau_{M+1})\end{pmatrix}=\begin{pmatrix}\mathcal{W}_M(\tau_1) & 0 & \dots & 0\\ 0 & \mathcal{W}_M(\tau_2) & \dots & 0\\ \vdots & \vdots & \ddots & \vdots\\ 0 & 0 & \dots & \mathcal{W}_M(\tau_{M+1})\end{pmatrix}\begin{pmatrix}\mathcal{W}_M(\tau_1)\\ \mathcal{W}_M(\tau_2)\\ \vdots\\ \mathcal{W}_M(\tau_{M+1})\end{pmatrix}=\breve{\boldsymbol{W}}\,\boldsymbol{W}.$$

On account of (3.2), we can write the matrix $\breve{\boldsymbol{W}}$ in the form

$$\breve{\boldsymbol{W}}=\breve{\boldsymbol{X}}\,\breve{\boldsymbol{K}}\,\breve{\boldsymbol{P}},$$

where

$$\breve{\boldsymbol{X}}:=\begin{pmatrix}\boldsymbol{\chi}_M(\tau_1) & 0 & \dots & 0\\ 0 & \boldsymbol{\chi}_M(\tau_2) & \dots & 0\\ \vdots & \vdots & \ddots & \vdots\\ 0 & 0 & \dots & \boldsymbol{\chi}_M(\tau_{M+1})\end{pmatrix},\quad \breve{\boldsymbol{K}}:=\begin{pmatrix}\boldsymbol{K}_M & 0 & \dots & 0\\ 0 & \boldsymbol{K}_M & \dots & 0\\ \vdots & \vdots & \ddots & \vdots\\ 0 & 0 & \dots & \boldsymbol{K}_M\end{pmatrix},\quad \breve{\boldsymbol{P}}:=\begin{pmatrix}\boldsymbol{P}_M & 0 & \dots & 0\\ 0 & \boldsymbol{P}_M & \dots & 0\\ \vdots & \vdots & \ddots & \vdots\\ 0 & 0 & \dots & \boldsymbol{P}_M\end{pmatrix}.$$

By repeating this process, one can easily find

$$\boldsymbol{W}^{2n+1}=\left(\breve{\boldsymbol{W}}\right)^{2n}\boldsymbol{W},\quad n\in\mathbb{N}. \tag{3.13}$$

With the aid of former approximation (3.13) and the preceding relations (3.5), (3.6), we set

$$\boldsymbol{H}:=\left\{-f\left(\boldsymbol{I}_M\,\boldsymbol{K}_M\,\boldsymbol{P}_M\right)\boldsymbol{X}_M\,(\boldsymbol{E}_M)^2+\boldsymbol{L}\left(\breve{\boldsymbol{W}}\right)^{2n}\boldsymbol{X}_M\right\}\boldsymbol{K}_M,$$

which is obtained by putting the relations (3.5)-(3.6) into the corresponding equation (3.12). We arrive at related fundamental matrix equation

$$\boldsymbol{H}\,\boldsymbol{P}_M = \boldsymbol{Z}, \qquad \text{or} \quad [\boldsymbol{H};\boldsymbol{Z}]. \tag{3.14}$$

3.1.3. Treatment of boundary conditions

The fundamental matrix equations for both linear and nonlinear models are obtained in the last parts. The implementations of boundary conditions have so far been left undone. We need to incorporate the related boundary conditions (1.1) and (1.2) into the matrix equations (3.10) and (3.14) respectively. We consider the relation (3.2) and tend $\tau \to 0, 1$ in order to implement the boundary conditions. In either case, we get

$$\begin{cases} \bar{\boldsymbol{H}}_0\,\boldsymbol{P}_M &= \omega_0, \quad \bar{\boldsymbol{H}}_0 := \boldsymbol{\chi}_M(0)\,\boldsymbol{K}_M, \\ \bar{\boldsymbol{H}}_1\,\boldsymbol{P}_M &= \omega_1, \quad \bar{\boldsymbol{H}}_1 := \boldsymbol{\chi}_M(1)\,\boldsymbol{K}_M. \end{cases} \tag{3.15}$$

Or equivalently we obtain two rows $[\bar{\boldsymbol{H}}_0;\omega_0]$ and $[\bar{\boldsymbol{H}}_1;\omega_1]$ to be added into the matrix equations. We now replace two rows of the fundamental matrix equations $[\boldsymbol{H};\boldsymbol{G}]$ in (3.10) or $[\boldsymbol{H};\boldsymbol{Z}]$ in (3.14) by two above new rows. Denote the modified matrix equations by $[\bar{\boldsymbol{H}};\bar{\boldsymbol{G}}]$ or $[\bar{\boldsymbol{H}};\bar{\boldsymbol{Z}}]$. In each case, by solving the modified equation we get the clique coefficients $p_0, p_1, \ldots, p_M$ for each model problem (1.1) or (1.2).

3.2. The quasilinearization approach

This part is devoted to applying first the common quasilinearization method (QLM) to the nonlinear and nonhomogeneous nonlocal model (1.2) to get a family of linearlized model equations. An analogue conclusion can be drawn for the model (I) as a special case of (II). The QLM has been successfully applied to many important nonlinear equations in the literature, we refer to [32–35] for more information.

Let by $\omega_s(\tau)$ we denote the quasilinear solution and $\omega_0(\tau)$ be a rough approximation to $\omega(\tau)$. Applying the QLM to the original nonlinear nonlocal model problem (1.2) we get the following

$$f\left(\int_0^1 \omega_s(p)dp\right)\frac{d^2}{d\tau^2}\omega_{s+1}(\tau) - \left[(2n+1)\ell(\tau)\,\omega_s^{2n}(\tau)\right]\omega_{s+1}(\tau) = -2n\,\ell(\tau)\,\omega_s^{2n+1}(\tau), \tag{3.16}$$

for $s = 1, 2, \ldots$. Note that during the QLM process we first assumed that the integral term $f\left(\int_0^1 \omega(p)dp\right)$ is a constant coefficient. Hence, we employed the QLM to the model and finally we replaced the unknown function $\omega(\tau)$ by the previous approximation $\omega_s(\tau)$. It should be emphasized that the initial approximation at $s = 0$ can not be taken as a zero function in $f\left(\int_0^1 \omega_s(p)dp\right)$. With the quasilinear model (3.16), the same boundary conditions as (1.2) are given

$$\omega_{s+1}(0) = \omega_1, \quad \omega_{s+1}(1) = \omega_1. \tag{3.17}$$

Remark 3.3. A similar technique can be applied to the first model problem (I) in (1.1) as a special case of model (II). In this case we get the following quasilinear models

$$\begin{cases} -f\left(\int_0^1 \omega_s(p)dp\right)\frac{d^2}{d\tau^2}\omega_{s+1}(\tau) = g(\tau), \\ \omega_{s+1}(0) = \omega_1, \quad \omega_{s+1}(1) = \omega_1. \end{cases} \qquad s = 1, 2, \ldots.$$

For simplicity of exposition, we utilize the following notations for the quasilinear models (3.16)

$$l_s(\tau) := -\left[(2n+1)\ell(\tau)\,\omega_s^{2n}(\tau)\right]/f\left(\int_0^1 \omega_s(p)dp\right), \quad g_s(\tau) := -2n\,\ell(\tau)\,\omega_s^{2n+1}(\tau)/f\left(\int_0^1 \omega_s(p)dp\right).$$

So, we may rewrite the equations (3.16) together with boundary conditions (3.17) into a concise form as

$$\begin{cases} \frac{d^2}{d\tau^2}\omega_{s+1}(\tau) + l_s(\tau)\,\omega_{s+1}(\tau) = g_s(\tau), \\ \omega_{s+1}(0) = \omega_1, \quad \omega_{s+1}(1) = \omega_1. \end{cases} \qquad s = 1, 2, \ldots. \tag{3.18}$$

We now apply the direct spectral clique collocation approach to the above family of equations. To this end, we suppose that the approximate solution $\mathcal{W}_{s,M}(\tau)$ to the true solution $\omega_s(\tau)$ of (3.18) is already computed in the iteration $s \geq 1$. In the next iteration and according to (3.1), we try to find a solution in terms of clique function as

$$\omega_{s+1}(\tau) \approx \mathcal{W}_{s+1,M}(\tau) = \sum_{m=0}^{M} p_m^{(s)} \mathbb{C}_m(\tau) = \boldsymbol{\chi}_M(\tau) \boldsymbol{K}_M \boldsymbol{P}_M^{(s)}, \quad \tau \in \Omega_\tau,$$

where we set $\boldsymbol{P}_M^{(s)} := \begin{bmatrix} p_0^{(s)} & p_1^{(s)} & p_2^{(s)} & \dots & p_M^{(s)} \end{bmatrix}^T$ and $\boldsymbol{\chi}_M(\tau)$, $\boldsymbol{K}_M$ are as defined in (3.1) or (2.3). We then proceed by placing the Chebyshev nodes (2.8) into (3.18). In the matrix format, we obtain

$$\boldsymbol{W}_{s+1}^{(2)} + \boldsymbol{L}_s \boldsymbol{W}_{s+1} = \boldsymbol{G}_s, \quad s = 1, 2, \dots, \quad \boldsymbol{G}_s = \begin{pmatrix} g_s(\tau_1) \\ g_s(\tau_2) \\ \vdots \\ g_s(\tau_{M+1}) \end{pmatrix}, \tag{3.19}$$

where

$$\boldsymbol{W}_{s+1} = \begin{pmatrix} \mathcal{W}_{s+1,M}(\tau_1) \\ \mathcal{W}_{s+1,M}(\tau_2) \\ \vdots \\ \mathcal{W}_{s+1,M}(\tau_{M+1}) \end{pmatrix}, \quad \boldsymbol{W}_{s+1}^{(2)} = \begin{pmatrix} \mathcal{W}_{s+1,M}^{(2)}(\tau_1) \\ \mathcal{W}_{s+1,M}^{(2)}(\tau_2) \\ \vdots \\ \mathcal{W}_{s+1,M}^{(2)}(\tau_{M+1}) \end{pmatrix}, \quad \boldsymbol{L}_s = \begin{pmatrix} l_s(\tau_1) & 0 & \dots & 0 \\ 0 & l_s(\tau_2) & \dots & 0 \\ \vdots & \vdots & \ddots & \vdots \\ 0 & 0 & \dots & l_s(\tau_{M+1}) \end{pmatrix}.$$

The results of Theorem 3.1 are also valid here, in the sense that

$$\boldsymbol{W}_{s+1} = \boldsymbol{X}_M \boldsymbol{K}_M \boldsymbol{P}_M^{(s)},$$
$$\boldsymbol{W}_{s+1}^{(2)} = \boldsymbol{X}_M (\boldsymbol{E}_M)^2 \boldsymbol{K}_M \boldsymbol{P}_M^{(s)}.$$

To get the linear fundamental matrix equation, it suffices to insert the proceeding relations into (3.19). Therefore, we arrive at

$$\boldsymbol{H}_s \boldsymbol{P}_M^{(s)} = \boldsymbol{G}_s, \qquad \text{or} \quad [\boldsymbol{H}_s; \boldsymbol{G}_s], \quad s = 1, 2, \dots, \tag{3.20}$$

where

$$\boldsymbol{H}_s := \left\{ \boldsymbol{X}_M (\boldsymbol{E}_M)^2 + \boldsymbol{L}_s \boldsymbol{X}_M \right\} \boldsymbol{K}_M.$$

To finalize the process, we require to implement the boundary conditions the matrix formats as we did before in (3.15) in the direct collocation technique. In this case, by replacing two rows of $[\boldsymbol{H}_s; \boldsymbol{G}_s]$ the resulting modified matrix equation will be denoted by $[\bar{\boldsymbol{H}}_s; \bar{\boldsymbol{G}}_s]$ for $s = 1, 2, \dots$. Based on solving this linear system the unknown clique coefficients are found. In contrast to the direct approaches previously described, we here just solve a linear algebraic system rather than a nonlinear one. We refer to the latter technique as QLM-clique scheme.

4. Implementation and graphical illustrations

A set of computational results is performed to show the accuracy of the presented direct and QLM-clique collocation matrix techniques and support the theoretical findings. The benefits of these attempts will be presented through comparisons of results in the model problems obtained by these matrix methods and the outcomes of other existing numerical techniques. All experimental simulations were conducted on an ASUS laptop computer with a 2.2 GHz Intel Core i7 CPU and 16 GB RAM. We utilized Matlab software version 2021a.

In order to measure the quality of approximations, the absolute error between the exact solution $\omega(\tau)$ and the numerical solutions $\mathcal{W}_M(\tau)$ and $\mathcal{W}_{s,M}(\tau)$ are defined as follows

$$\mathcal{E}_M(\tau) := \left|\omega(\tau) - \mathcal{W}_M(\tau)\right|, \quad \mathcal{E}_{s,M}(\tau) := \left|\omega(\tau) - \mathcal{W}_{s,M}(\tau)\right|, \quad \tau \in \Omega_\tau. \tag{4.1}$$

We also calculate the norms (for a fixed s) of the former error terms (4.1) as follows

$$\mathbb{E}_\infty \equiv \mathbb{E}_\infty(M) := \max_{\tau \in \Omega_\tau} \mathcal{E}_M(\tau), \quad \mathbb{E}_{s,\infty} \equiv \mathbb{E}_{s,\infty}(M) := \max_{\tau \in \Omega_\tau} \mathcal{E}_{s,M}(\tau).$$

The following expressions are further used to calculate the obtained order of convergence (OC) related to both numerical techniques given by

$$\mathrm{OC}_\infty := \log_2 \left(\frac{\mathbb{E}_\infty(M)}{\mathbb{E}_\infty(2M)} \right), \quad \mathrm{OC}_{s,\infty} := \log_2 \left(\frac{\mathbb{E}_{s,\infty}(M)}{\mathbb{E}_{s,\infty}(2M)} \right). \tag{4.2}$$

Table 1
Numerical/exact solutions in Test Example 4.1 with $M = 3$ and diverse $\tau \in \Omega_\tau$.

x	Clique			VIM [4]	
	$\mathcal{W}_3(\tau)$	Exact	$\mathcal{E}_3(\tau)$	u_{10}	AE
0.1	0.000999999999958	0.001	$4.1654014 \times 10^{-14}$	0.0010252914	2.5×10^{-5}
0.2	0.007999999999917	0.008	$8.3121066 \times 10^{-14}$	0.0080490501	4.9×10^{-5}
0.3	0.026999999999879	0.027	$1.2068369 \times 10^{-13}$	0.0270697430	7.0×10^{-5}
0.4	0.063999999999849	0.064	$1.5106849 \times 10^{-13}$	0.0640858376	8.6×10^{-5}
0.5	0.124999999999829	0.125	$1.7100210 \times 10^{-13}$	0.1250958009	9.6×10^{-5}
0.6	0.215999999999823	0.216	$1.7721113 \times 10^{-13}$	0.2160981001	9.8×10^{-5}
0.7	0.342999999999834	0.343	$1.6642221 \times 10^{-13}$	0.3430912024	9.1×10^{-5}
0.8	0.511999999999865	0.512	$1.3536194 \times 10^{-13}$	0.5120735751	7.4×10^{-5}
0.9	0.728999999999919	0.729	$8.0756957 \times 10^{-14}$	0.7290436852	4.4×10^{-5}

Test example 4.1. The first test case is devoted to a non-homogeneous model in the form (1.1) as given by [4,10,11]

$$\left(\int_0^1 \omega(p)dp\right)^{1/3} \frac{d^2}{d\tau^2}\omega(\tau) = \frac{6\tau}{4^{1/3}}, \quad \tau \in \Omega_\tau,$$

and with the boundary conditions $\omega(0) = 0$ and $\omega(1) = 1$. One can verify that the true solution is $\omega(\tau) = \tau^3$.

For this example, we set $M = 3$ and use the direct clique-collocation approach (3.10). By using the four collocation points $\{321/8434, 467/1513, 1046/1513, 1567/1629\}$ and solving the modified fundamental matrix equation $[\bar{\boldsymbol{H}}; \bar{\boldsymbol{G}}]$ we get the unknown coefficients as

$$\boldsymbol{P}_3 = \left(1.0, 3.0, -3.0, 1.0\right)^T.$$

Hence, the approximate solution is obtained by considering the clique vector $\boldsymbol{C}_3(\tau)$ as

$$\mathcal{W}_3(\tau) = \boldsymbol{C}_3(\tau)\boldsymbol{P}_3 = \begin{pmatrix} 1 & 1+\tau & 1+2\tau+\tau^2 & 1+3\tau+3\tau^2+\tau^3 \end{pmatrix} \begin{pmatrix} 1 \\ 3 \\ -3 \\ 1 \end{pmatrix} = \tau^3,$$

which is clearly the exact solution. Note that the required CPU time for $M = 3$ by the direct clique collocation method is about 2 seconds. We also notice that the measured time is taken to solve the final fundamental matrix equation (3.20).

For further validation, a comparison is made between the numerical outcomes gained by the direct collocation technique (3.10) and the results obtained via the variational iteration method (VIM) [4] with 10 iterations in Table 1. The numerical results are obtained with $M = 3$ and evaluated at some points $\tau \in [0, 1]$. The exact solutions are also tabulated in the third column. Note that the last column shows the absolute errors (AE) achieved by VIM. It can be readily observed that the present technique with a lower computational cost performs extremely better than VIM.

Test example 4.2. We now consider the homogeneous model in the form (1.2). By taking $f(t) = \frac{1}{t}$ and $n = 2$, we have the following model [4,10,11]

$$-\left(\int_0^1 \omega(p)dp\right)^{-1} \frac{d^2}{d\tau^2}\omega(\tau) + \frac{3}{8(\sqrt{2}-1)}\omega^5(\tau) = 0, \quad \tau \in \Omega_\tau.$$

The given boundary conditions are $\omega(0) = 1$ and $\omega(1) = \frac{1}{\sqrt{2}}$. The exact solution is given by $\omega(\tau) = \frac{1}{\sqrt{\tau+1}}$.

We first set $M = 5$. Using the direct clique collocation approach (3.14), we get the approximate solution

$$\mathcal{W}_5(\tau) = -0.02973645463\,\tau^5 + 0.1247582345\,\tau^4 - 0.2506226733\,\tau^3 + 0.3614999396\,\tau^2 - 0.498792265\,\tau + 1.0.$$

Utilizing the same number of clique bases, we employ the second linearized QLM-clique technique with $s = 5$ and the initial approximation $\omega_0(\tau) = 1 - \tau/2$. The obtained approximation is

$$\mathcal{W}_{5,5}(\tau) = -0.02973645162\,\tau^5 + 0.124758223\,\tau^4 - 0.2506226538\,\tau^3 + 0.3614999168\,\tau^2 - 0.4987922532\,\tau + 1.0.$$

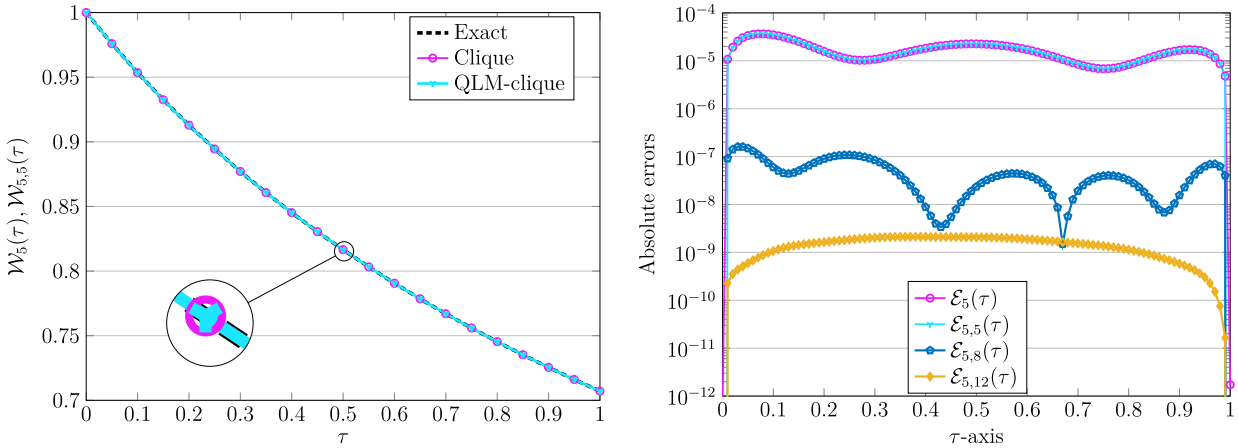

Fig. 1. Approximate solutions versus exact one obtained via clique/QLM-clique collocation approach (left) and the associated absolute errors (right) in Test Example 4.2 with $M = 5, 8, 12$, and $s = 5$.

It is evident that the coefficients of both solutions are coincided up to 8 number of digits. To see the effect of using different initial approximations, we take $\omega_0(\tau) = 1$. In this case, we get

$$\mathcal{W}_{5,5}(\tau) = -0.02973644636\,\tau^5 + 0.1247582027\,\tau^4 - 0.2506226196\,\tau^3 + 0.3614998768\,\tau^2 - 0.4987922323\,\tau + 1.0,$$

which is approximately the same as the last one.

The profile of approximate solutions $\mathcal{W}_5(\tau)$ and $\mathcal{W}_{5,5}(\tau)$ together with related exact solution are depicted in Fig. 1, the left picture. The related achieved absolute errors obtained via both approaches are also depicted in the same figure, the right part. We emphasize that we can obtain more accuracy by increasing M. To justify this fact, we use $M = 8$ and $M = 12$ in the QLM-clique technique. The achieved absolute errors for two latter values of M are also depicted in Fig. 1.

To validate the obtained result, let us mention the following approximate solution obtained via the combined Green's function and optimal homotopy analysis method GF-OHAM [10,11]

$$\phi_2(x) = 1 - 0.4973\,x + 0.3737\,x^2 - 0.3060\,x^3 + 0.2235\,x^4 - 0.1258\,x^5 + 0.05148\,x^6 - 0.0153\,x^7 + 0.0033\,x^8 - 0.00055\,x^9 + 0.0000646\,x^{10} \ldots.$$

The corresponding approximation attained via QLM-clique with $M = 10$ is given by

$$\mathcal{W}_{5,10}(\tau) = 1.0 - 0.4999995\,\tau + 0.37498269\,\tau^2 - 0.31223646\,\tau^3 + 0.2712800\,\tau^4 - 0.23535132\,\tau^5 + 0.19050825\,\tau^6 - 0.13024817\,\tau^7 + 0.066533613\,\tau^8 - 0.0216455\,\tau^9 + 0.0032831897\,\tau^{10}.$$

Note, the same result is obtained by the direct clique approach, but we omit it to save space. These approximate solutions can also be compared with the series expansion of the exact solution given by

$$\omega(\tau) = \frac{1}{\sqrt{\tau+1}} \approx 1 - \frac{1}{2}\tau + \frac{3}{8}\tau^2 - \frac{5}{16}\tau^3 + \frac{35}{128}\tau^4 - \ldots.$$

Table 2 shows some comparisons with two available existing numerical procedures. For this purpose, we use the VIM [4] and the GF-OHAM [10].

In the next simulation results, we compare the performance of two proposed matrix algorithms in terms of efficiency and numerical order of convergence (OC). To this end, different values of $M = 2^j$, $j = 0, 1, 2, 3, 4$ are utilized. The error norms $\mathbb{E}_\infty$ and $\mathbb{E}_{s,\infty}$ for $s = 5$ related to test Example 4.2 are tabulated in Table 3. The spent CPU times measured in seconds are further presented in this table. Besides, the estimated OC for these error norms are shown in Table 3. Let us emphasize that we could not obtain reasonable outcomes in the direct approach for $M = 16$, so we have not reported the results in this case. It can be obviously realized that the estimated OC of both matrix collocation strategies has exponential behavior as proved in Theorem 2.1. However, the CPU times reported in Table 3 show that the QLM-clique matrix algorithm is more efficient than the direct collocation approach.

Test example 4.3. In the third test study we again consider to the homogeneous model with $f(t) = \frac{1}{t^2}$ and $n = 1$ in the form (1.2). Thus, we get [10,11]

Table 2
Numerical/exact solutions in Test Example 4.2 utilizing $M = 5$ and diverse $\tau \in \Omega_\tau$.

x	QLM-clique			VIM [4]		GF-OHAM [10]	
	$\mathcal{W}_{5,5}(\tau)$	Exact	$\mathcal{E}_5(\tau)$	u_3	AE	ϕ_2	E_2
0.1	0.953497330	0.953462589245592	3.47×10^{-5}	0.9535746906	1.1×10^{-4}	0.953715758	2.53×10^{-4}
0.2	0.912886662	0.912870929175277	1.57×10^{-5}	0.9130017937	1.3×10^{-4}	0.913348055	4.77×10^{-4}
0.3	0.877068787	0.877058019307029	1.08×10^{-5}	0.8773763380	3.2×10^{-4}	0.877702187	6.44×10^{-4}
0.4	0.845172545	0.845154254728517	1.83×10^{-5}	0.8454589061	3.0×10^{-4}	0.845886767	7.32×10^{-4}
0.5	0.816519146	0.816496580927726	2.26×10^{-5}	0.8167992837	3.0×10^{-4}	0.817233417	7.36×10^{-4}
0.6	0.790586484	0.790569415042095	1.71×10^{-5}	0.7909250558	3.6×10^{-4}	0.791235825	6.66×10^{-4}
0.7	0.766973456	0.766964988847370	8.47×10^{-6}	0.7672832340	3.2×10^{-4}	0.767504100	5.39×10^{-4}
0.8	0.745364273	0.745355992499930	8.28×10^{-6}	0.7457397214	3.8×10^{-4}	0.745731089	3.75×10^{-4}
0.9	0.725492783	0.725476250110012	1.65×10^{-5}	0.7257126136	2.3×10^{-4}	0.725667948	1.91×10^{-4}

Table 3
The results of maximum absolute error norms, the corresponding estimated order of convergence, and CPU times, in Test Example 4.2 with diverse M.

M	Clique			QLM-clique		
	$\mathbb{E}_\infty$	OC_∞	CPU(s)	$\mathbb{E}_{5,\infty}$	$\mathrm{OC}_{5,\infty}$	CPU(s)
1	3.7814×10^{-2}	–	0.29995	3.7814×10^{-2}	–	0.37005
2	6.4447×10^{-3}	2.5527	0.83433	6.4447×10^{-3}	2.5527	0.41440
4	2.0937×10^{-5}	4.9440	2.90217	2.0938×10^{-4}	4.9440	0.50689
8	1.5987×10^{-7}	10.355	15.5894	1.6031×10^{-7}	10.351	0.72272
16	–	–	–	2.1024×10^{-9}	6.2527	1.30033

$$-\left(\int_0^1 \omega(p)dp\right)^{-2} \frac{d^2}{d\tau^2}\omega(\tau) + \left(\frac{\sqrt{2}}{\ln 2}\right)^2 \omega^3(\tau) = 0, \quad \tau \in \Omega_\tau.$$

The accompanied boundary conditions given as $\omega(0) = 1$ and $\omega(1) = \frac{1}{2}$. Here, the function $\omega(\tau) = \frac{1}{\tau+1}$ is known as the exact solution to this model.

The approximate solutions using $M = 8$ via the direct clique and QLM-clique matrix collocation procedures obtained as follows respectively

$$\mathcal{W}_8(\tau) = 0.03299843825\,\tau^8 - 0.182257207\,\tau^7 + 0.4642505855\,\tau^6 - 0.7525294686\,\tau^5 + 0.9251400828\,\tau^4 - 0.9863217331\,\tau^3 + 0.9986653453\,\tau^2 - 0.9999460432\,\tau + 1.0,$$

and

$$\mathcal{W}_{5,8}(\tau) = 0.032985326\,\tau^8 - 0.18218723\,\tau^7 + 0.46408212\,\tau^6 - 0.75228112\,\tau^5 + 0.92487946\,\tau^4 - 0.98610858\,\tau^3 + 0.99851115\,\tau^2 - 0.99988113\,\tau + 1.0.$$

Note that in the latter QLM-clique solution, we have used the initial approximation $\omega_0(\tau) = 1 - \tau$ and $s = 5$ was taken as before. Clearly, one sees a good alignment between the given coefficients. The graphical illustrations of the foregoing approximations are shown in Fig. 2. Besides, the graphics of related absolute errors $\mathcal{E}_8(\tau)$ and $\mathcal{E}_{5,8}(\tau)$ are presented in this figure.

Similar to the second test case, we compare the result of the proposed method with the result reported via GF-OHAM. The approximate solution obtained by this scheme is [10,11]

$$\phi_2(x) = 1 - 1.00399\,x + 0.995127\,x^2 - 0.90086\,x^3 + 0.655261\,x^4 - 0.338986\,x^5 + 0.115228\,x^6 - 0.0246916\,x^7 + 0.00308645\,x^8 - 0.00017147\,x^9 \ldots.$$

In Table 4, a comparison between $\mathcal{W}_{5,5}(\tau)$ and the above solution ϕ_2 evaluated at some point $\tau \in \Omega_\tau$ is reported. Additionally, the associated absolute errors $\mathcal{E}_{5,5}(\tau)$ and $E_2 = |u - \phi_2|$ are presented in Table 4. Obviously, the obtained solution of degree 5 is more accurate than the approximation of degree 9 obtained by using the GF-OHAM [10,11].

Indeed, the approximate solution using $M = 9$ obtained by utilizing the QLM-clique scheme is given by

$$\mathcal{W}_{5,9}(\tau) = 1.0 - 0.99992353\,\tau + 0.99949587\,\tau^2 - 0.99536662\,\tau^3 + 0.9698158\,\tau^4 - 0.87685961\,\tau^5 + 0.66908189\,\tau^6 - 0.38018454\,\tau^7 + 0.13663536\,\tau^8 - 0.022694623\,\tau^9.$$

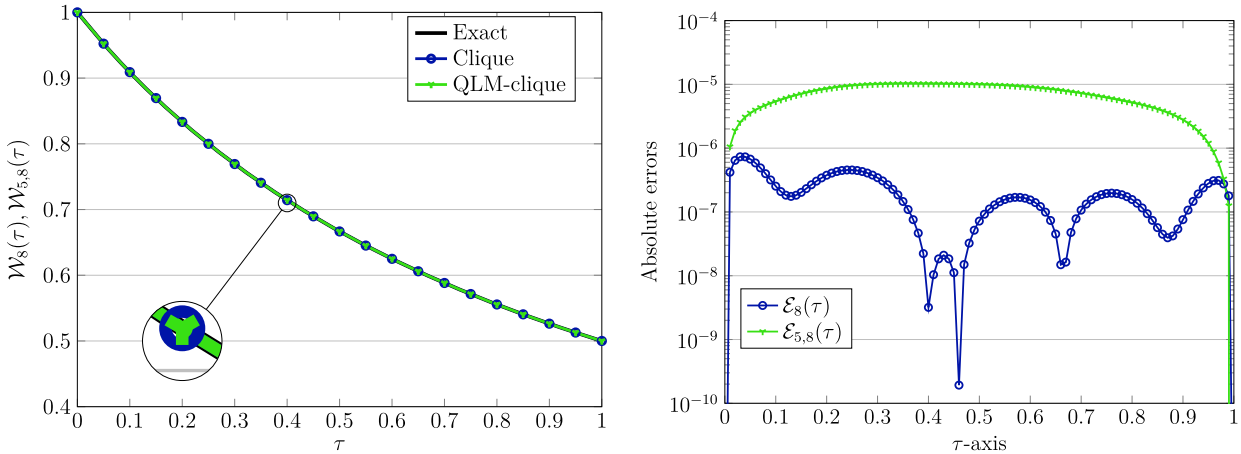

Fig. 2. Approximate solutions versus exact one obtained via clique/QLM-clique collocation approach (left) and the associated absolute errors (right) in Test Example 4.3 with $M = 8$, and $s = 5$.

Table 4
Numerical/exact solutions in Test Example 4.3 with $M = 5$ and diverse $\tau \in \Omega_\tau$.

x	QLM-clique			GF-OHAM [10,11]	
	$\mathcal{W}_{5,5}(\tau)$	Exact	$\mathcal{E}_{5,5}(\tau)$	ϕ_2	E_2
0.1	0.909221629705822	0.909090909090909	1.3072×10^{-4}	0.908713383	3.77×10^{-4}
0.2	0.833390455620759	0.833333333333333	5.7122×10^{-5}	0.832746652	5.86×10^{-4}
0.3	0.769267982919968	0.769230769230769	3.7214×10^{-5}	0.768603045	6.27×10^{-4}
0.4	0.714350231166983	0.714285714285714	6.4517×10^{-5}	0.713705107	5.80×10^{-4}
0.5	0.666746826500040	0.666666666666667	8.0160×10^{-5}	0.666157571	5.09×10^{-4}
0.6	0.625060093818403	0.625000000000000	6.0094×10^{-5}	0.624561470	4.38×10^{-4}
0.7	0.588264148968677	0.588235294117647	2.8855×10^{-5}	0.587870965	3.64×10^{-4}
0.8	0.555583990931140	0.555555555555556	2.8435×10^{-5}	0.555285414	2.70×10^{-4}
0.9	0.526374594006055	0.526315789473684	5.8805×10^{-5}	0.526170109	1.45×10^{-4}

Table 5
The results of maximum absolute error norms, the corresponding estimated order of convergence, and CPU times in Test Example 4.3 with diverse M.

M	Clique			QLM-clique		
	$\mathbb{E}_\infty$	OC_∞	CPU(s)	$\mathbb{E}_{5,\infty}$	$\mathrm{OC}_{5,\infty}$	CPU(s)
1	8.5780142×10^{-2}	–	0.31551	8.5780142×10^{-2}	–	0.38790
2	1.7280180×10^{-2}	2.3115	1.46497	1.7283500×10^{-2}	2.3112	0.43169
4	7.1513421×10^{-4}	4.5948	3.39733	7.1999405×10^{-4}	4.5853	0.51555
8	7.3183300×10^{-7}	9.9325	54.0007	1.0248915×10^{-5}	6.1344	0.70158

On the other hand, the Maclaurin series form of the exact solution is $\omega(\tau) = 1 - \tau + \tau^2 - \tau^3 + \ldots$. By looking at these solutions, we can easily conclude that the proposed approach has more accuracy than the other one.

Finally, the results of maximum absolute error norms as well as the elapsed CPU time (in seconds) related to both presented approaches are provided in Table 5. Along with these errors, we report the estimated OC. The results show that by increasing M the accuracy of the direct method is better than the QLM-clique procedure. However, as shown before, the latter approach is more efficient than the direct procedure especially when we use a larger problem size. For example for $M = 8$ the time needed for the direct clique collocation is about eight times longer than the QLM-clique matrix method.

5. Conclusions

This study has proposed two matrix collocation techniques that rest upon (novel) clique functions of graphs for solving two classes of nonlinear, nonlocal, and two-point boundary value problems (BVPs). The first algorithm applied directly to the model problems while in the second approach, the given equation was first transformed into a sequence of quasilinear equations followed by solving them via the former direct algorithm. The convergence of the clique basis function is verified in a weighted L_2 norm. The presented algorithms are applied to solve numerically three test examples with known true solutions for their order of convergence. The main achievements of the current study can be summarized in the following points:

- The proposed direct clique matrix collocation approach is more accurate than two existing numerical procedures such as VIM [4] and GF-HAM [10].
- The second QLM-clique matrix methodology as a combination of the quasilinearization and the direct matrix method is not only accurate but also computationally efficient in terms of elapsed CPU time, see Tables 2 and 5.
- Besides, the outcomes presented in tables and figures show that both methods are exponentially convergent, which confirms the theoretical upper bound derived in Theorem 2.1.

The presented numerical approaches can be easily extended to solve diverse types of BVPs in science and engineering.

CRediT authorship contribution statement

Mohammad Izadi: Conceptualization, Investigation, Methodology, Software, Validation, Visualization, Writing – original draft, Writing – review & editing. **Jagdev Singh:** Formal analysis, Validation, Writing – review & editing. **Samad Noeiaghdam:** Validation, Writing – review & editing.

Declaration of competing interest

The authors declare that they have no known competing financial interests or personal relationships that could have appeared to influence the work reported in this paper.

Data availability

No data was used for the research described in the article.

Funding

There is no funding.

References

[1] Y. Lin, J.A. Enszer, M.A. Stadtherr, Enclosing all solutions of two-point boundary value problems for ODEs, Comput. Chem. Eng. 32 (8) (2008) 1714–1725.
[2] W.E. Boyce, R.C. DiPrima, D.B. Meade, Elementary Differential Equations and Boundary Value Problems, John Wiley & Sons, 2021.
[3] J.R. Cannon, D.J. Galiffa, A numerical method for a nonlocal elliptic boundary value problem, J. Integral Equ. Appl. 20 (2) (2008) 243–261.
[4] S. Khuri, A.M. Wazwaz, A variational approach for a class of nonlocal elliptic boundary value problems, J. Math. Chem. 52 (5) (2014) 1324–1337.
[5] J.R. Cannon, D.J. Galiffa, On a numerical method for a homogeneous, nonlinear, nonlocal, elliptic boundary value problem, Nonlinear Anal. 74 (5) (2011) 1702–1713.
[6] W. Themistoclakis, A. Vecchio, On the numerical solution of some nonlinear and nonlocal boundary value problems, Appl. Math. Comput. 255 (2015) 135–146.
[7] A. Luongo, G. Piccardo, Non-linear galloping of sagged cables in 1: 2 internal resonance, J. Sound Vib. 214 (5) (1998) 915–940.
[8] J.W. Bebernes, A.A. Lacey, Shear band for a non-local model of thermo-viscoelastic flows, Adv. Math. Sci. Appl. 15 (2005) 265–282.
[9] R. Stánczy, Nonlocal elliptic equations, Nonlinear Anal. 47 (5) (2001) 3579–3584.
[10] R. Singh, An iterative technique for solving a class of local and nonlocal elliptic boundary value problems, J. Math. Chem. 198 (2020) 105781.
[11] H. Singh, An efficient technique based on the HAM with Green's function for a class of nonlocal elliptic boundary value problems, Comput. Methods Differ. Equ. 9 (2021) 722–735.
[12] H. Singh, Solving a class of local and nonlocal elliptic boundary value problems arising in heat transfer, Heat Transf. 51 (2022) 1524–1542.
[13] M. Izadi, Ş. Yüzbaşı, W. Adel, Accurate and efficient matrix techniques for solving the fractional Lotka-Volterra population model, Physica A 600 (2022) 127558.
[14] Z.A. Noor, I. Talib, T. Abdeljawad, M.A. Alqudah, Numerical study of Caputo fractional-order differential equations by developing new operational matrices of Vieta-Lucas polynomials, Fractal Fract. 6 (2) (2022) 79.
[15] M. Izadi, A combined approximation method for nonlinear foam drainage equation, Sci. Iran. 29 (1) (2022) 70–78.
[16] S.S. Ahmed, S.J. MohammedFaeq, Bessel collocation method for solving Fredholm-Volterra integro-fractional differential equations of multi-high order in the Caputo sense, Symmetry 13 (12) (2021) 2354.
[17] M. Izadi, Ş. Yüzbaşı, W. Adel, Two novel Bessel matrix techniques to solve the squeezing flow problem between infinite parallel plates, Comput. Math. Math. Phys. 61 (12) (2021) 2034–2053.
[18] K.D. Dwivedi, J. Singh, Numerical solution of two-dimensional fractional-order reaction advection sub-diffusion equation with finite-difference Fibonacci collocation method, Math. Comput. Simul. 181 (2021) 38–50.
[19] Y.H. Youssri, R.M. Hafez, Exponential Jacobi spectral method for hyperbolic partial differential equations, Math. Sci. 13 (4) (2019) 347–354.
[20] M. Izadi, A computational algorithm for simulating fractional order relaxation-oscillation equation, SeMA J. 79 (4) (2022) 647–661.
[21] M. Razavi, M.M. Hosseini, A. Salemi, Error analysis and Kronecker implementation of Chebyshev spectral collocation method for solving linear PDEs, Comput. Methods Differ. Equ. 10 (4) (2022) 914–927.
[22] Y. Öztürk, Numerical solution of systems of differential equations using operational matrix method with Chebyshev polynomials, J. Taibah Univ. Sci. 12 (2) (2018) 155–162.
[23] M. Izadi, P. Roul, A highly accurate and computationally efficient technique for solving the electrohydrodynamic flow in a circular cylindrical conduit, Appl. Numer. Math. 181 (2022) 110–124.
[24] D. Baleanu, B. Shiri, H.M. Srivastava, M. Al Qurashi, A Chebyshev spectral method based on operational matrix for fractional differential equations involving non-singular Mittag-Leffler kernel, Adv. Differ. Equ. 2018 (2018) 353.
[25] Z. Abbasi, M. Izadi, M.M. Hosseini, A highly accurate matrix method for solving a class of strongly nonlinear BVP arising in modeling of human shape corneal, Math. Methods Appl. Sci. 46 (2) (2023) 1511–1527.
[26] S. Kumbinarasaiah, A new approach for the numerical solution for the non-linear Klein–Gordon equation, SeMA J. 77 (2020) 435–456.

[27] W. Adel, S. Kumbinarasaiah, A new clique polynomial approach for fractional partial differential equations, Int. J. Nonlinear Sci. Numer. Simul. (2022), https://doi.org/10.1515/ijnsns-2021-0258.
[28] S. Kumbinarasaiah, M.P. Preetham, A study on homotopy analysis method and clique polynomial method, Comput. Methods Differ. Equ. 10 (3) (2022) 774–788.
[29] W.D. Wallis, A Beginner's Guide to Graph Theory, Springer Science & Business Media, 2007.
[30] C. Hoede, X. Li, Clique polynomials and independent set polynomials of graphs, Discrete Math. 125 (1994) 219–228.
[31] G.W. Stewart, Afternotes on Numerical Analysis, vol. 49, SIAM, 1996.
[32] M. Izadi, H.M. Srivastava, Generalized Bessel quasilinearlization technique applied to Bratu and Lane-Emden type equations of arbitrary order, Fractal Fract. 5 (4) (2021) 179.
[33] F. Zare, M. Heydari, G.B. Loghmani, Quasilinearization-based Legendre collocation method for solving a class of functional Volterra integral equations, Asian-Eur. J. Math. 16 (05) (2023) 2350078.
[34] B. Hu, Z. Wang, M. Xu, D. Wang, Quasilinearization method for an impulsive integro-differential system with delay, Math. Biosci. Eng. 19 (1) (2022) 612–623.
[35] M. Izadi, Ş. Yüzbaşı, S. Noeiaghdam, Approximating solutions of non-linear Troesch's problem via an efficient quasi-linearization Bessel approach, Mathematics 9 (16) (2021) 1841.